Paper presented at IEEE, Nuclear Science Symposium
Anaheim, November 2-4

TRI-PP-96-59
Oct 1996

A Count Rate Model for PET and its Application to an LSO HR PLUS Scanner

C. Moisan, J.G. Rogers, and J. L. Douglas
TRIUMF, 4004 Wesbrook Mall, Vancouver B.C., Canada V6T 2A3

Abstract

We present a count rate model for PET. Considering a standard 20×20 cm phantom in the field-of-view of a cylindrical septaless tomograph, the model computes the acceptance to prompt and random events from simple geometric considerations. Dead time factors at all stages of a typical event acquisition architecture are calculated from specified processing clock cycles. Validations of the model's predictions against the measured performances of the ECAT-953B and the EXACT HR PLUS are presented. The model is then used to investigate the benefit of using detectors made of LSO in the EXACT HR PLUS scanner geometry. The results indicate that in replacing BGO by the faster LSO, one can count on an increase of the peak noise-equivalent-count rate by a factor 2.2. This gain will be achieved by using a 5 nsec coincidence window, buckets operating on a 128 nsec clock cycle, and a front-end data acquisition that can sustain a total rate of 2.9 MHz.

I. Introduction

Lutetium oxyorthosilicate (LSO) has bulk characteristics that are comparable to those of BGO but with the advantages of a 40 nsec decay time and a light yield 5 times greater. Detectors made of this scintillator therefore offers to positron emission tomography (PET) the promises of reduced dead time losses and improved suppression of the random and scatter backgrounds. We present here a model developed to evaluate the benefit of using LSO detectors on the count rate characteristics of state-of-the-art PET scanners.

In the first part of this paper we briefly develop our model. As it only questions potential improvements to count rate performances, the treatment is restricted from the onset to septaless annular cameras with a cylindrical phantom of activity in the field-of-view (FOV). Born out of geometrical considerations, the formalism has the merit of its simplicity compared to previous analytical work [1]. Compared to detailed Monte Carlo simulations it also advantageously preserves an explicit dependence of the various count rate components upon the tomograph geometry. Also, at variance with previous work in [2], the model accounts for dead time losses by relying on the tomograph specifications as opposed to fitted effective values. This allows us to investigate the impact of modifications to the timing specifications at each level of the data processing chain while implementing LSO detectors. As a validation, the model is then shown to reproduce to a good accuracy the measured count rate performances of the ECAT-953B and EXACT HR PLUS scanners manufactured by Siemens-CTI. Finally, in the second part of the paper, the validated model is used to quantify the relative gain of using LSO detectors on the noise-equivalent-count (NEC) rate of the EXACT HR PLUS scanner.

II. A Count Rate Model

A. *The Rates of Single and True Events*

Considering a uniformly active water filled phantom, the rates of single and true events in the acceptance of a septaless ring tomograph can be estimated from simple geometrical considerations. Given a unit detection element, $d\Omega$, on the tomograph's surface, these rates can be expressed as the product of: the number of photons emitted per unit solid angle, a detection efficiency, ϵ_d, the specific activity of the phantom, A, and the fraction of the phantom's volume in view of that element, V_Ω. For a phantom of radius R_{PH} and length L_{PH}, V_Ω is the product of the cross section of the phantom, πR_{PH}^2, and a length. This length is fixed by the requirement that the unit detection element operates in single or coincidence mode and is easily shown to be equal to L_{PH} or $Z_d/2$ for singles and trues respectively. These expressions will hold true provided the phantom's length is in the range $Z_d \leq L_{PH} \leq 2Z_dR_d/(R_d - R_e)$, where Z_d, R_d and R_e are the tomograph's axial length, ring radius and end-shield radius. Integrating over the tomograph's solid angle then yields the following total single, $\hat{N}_s(\epsilon_d)$, and true, $\hat{N}_t(\epsilon_d)$, rates:

$$\hat{N}_s(\epsilon_d) = \frac{2}{4\pi}\epsilon_d A\left(\pi R_{PH}^2 L_{PH}\right)\left(\frac{2\pi Z_d}{R_d}\right), \quad (1)$$

$$\hat{N}_t(\epsilon_d) = \frac{1}{2\pi}\epsilon_d^2 A\left(\pi R_{PH}^2 Z_d/2\right)\left(\frac{\pi Z_d}{R_d}\right). \quad (2)$$

Scattering in the phantom volume or the tomograph material may be accounted for at this stage by the introduction of survival probabilities for the photons. These correction factors are computed as the average ratio of single or true events surviving their passage through the phantom volume or tomograph passive material to those expected in absence of any attenuation. The single and true rates then become:

$$N_s(\epsilon_d) = (P_s^0 + P_s^1)\dot{N}_s(\epsilon_d)\,, \quad (3)$$

$$N_t(\epsilon_d) = (P_t^0 + P_t^1)\dot{N}_t(\epsilon_d)\,, \quad (4)$$

$$= N_{unscatt}(\epsilon_d) + N_{scatt}(\epsilon_d)\,. \quad (5)$$

For single events, P_s^0 and P_s^1 are respectively the probabilities that a single photon will be detected after undergoing none or at least one Compton interaction. Similarly for the trues, P_t^0 and P_t^1 are the probabilities that none or at least one photon underwent a scattering interaction before reaching the detectors. For convenience, the trues are also expressed as the sum of separate contributions for unscattered and scattered events. Values for these factors can be obtained either analytically or through Monte Carlo techniques. The method used here for their evaluation will be detailed in Section D.

B. The Rates of Randoms and Multiples

Random events occur when two uncorrelated singles are detected in the resolving time of a coincidence window. Their rate depends on the single rate in each detector and on the number of pairs of detectors accepted by the coincidence logic. In state-of-the-art tomographs, detectors are grouped into so called buckets. The FOV is defined by the condition that any of the n_{buck} buckets may be in coincidence with all the others except for itself and a number, $n_{excl} - 1$, of immediately adjacent neighbors. The rate of random coincidences is accordingly:

$$N_r(\epsilon_d) = \tau_{coinc}\left(\frac{N_s(\epsilon_d)}{n_{buck}}\right)^2 n_{pair}\,, \quad (6)$$

where τ_{coinc} is the coincidence window width, and n_{pair} is the number of bucket pairs allowed in the FOV:

$$n_{pair} = \frac{n_{buck}(n_{buck} - n_{excl})}{2}. \quad (7)$$

Multiple events, may also be acquired when an uncorrelated single is in coincidence with two photons from a true event, (s+t), or those from a random, (s+r). Their respective rates are given by:

$$N_{s+i}(\epsilon_d) = \tau_{coinc}\frac{N_i(\epsilon_d)}{n_{pair}} \times \frac{N_s(\epsilon_d)}{n_{buck}} n_{tripl}\,, \quad (8)$$

where the label i stands for either trues or randoms, and n_{tripl} is the total number of bucket triplets allowed by the coincidence logic of the scanner.

C. Dead Time Losses

In modern tomographs single events may first be lost at the block detector level. At moderate rates, singles can be lost if they interact within the fixed time, τ_{block}, taken to integrate the energy signal left by a previous event. At high incoming rates, two or more singles may also pile-up within a time much smaller than τ_{block} to paralyse the block. Single events are secondly lost at the bucket level. Each detector has a dedicated input channel to present its events to a given bucket, which in turn will arbitrate between all busy channels to output only one event in a processing time period of τ_{buck}. These losses are introduced in our model by scaling down the intrinsic detection efficiency, ϵ_d, such that:

$$\epsilon_d \rightarrow \epsilon'_d = \epsilon_d \epsilon_{thr} \times \frac{\exp(-\tau_{block} N_s(\epsilon_d)/n_{block})}{1 + \tau_{block} N_s(\epsilon_d)/n_{block}}\,, \quad (9)$$

$$\epsilon'_d \rightarrow \epsilon''_d = \epsilon'_d \times \frac{1}{1 + \tau_{buck} N_s(\epsilon'_d) n_{blbk}/n_{block}}. \quad (10)$$

In the previous equations, $N_s(\epsilon_d)$ is th scatter corrected single rate from equation (3), while the efficiency ϵ_{thr} is introduced to possibly account for thresholding and/or the packing gaps between adjacent blocks.

Event losses will also occur when more than one true or random events collide at the coincidence processor during the same time interval, τ_{proc}. If the total rate out of the coincidence processor exceeds a finite bandwidth, N_{BWL}, events will also be lost due to saturation of the front-end data acquisition system. To account for losses at the final levels of the data processing architecture, the true and random rates presented to and exiting from the coincidence processor are respectively scaled down according to:

$$n_i(\epsilon''_d) = \frac{N_i(\epsilon''_d)}{1 + \tau_{proc} N_{tot}(\epsilon''_d)/n_{proc}}\,, \quad (11)$$

$$n'_i(\epsilon''_d) = n_i(\epsilon''_d)\frac{N_{BWL}}{\sum_i n_i(\epsilon''_d)} \text{ if } \sum_i n_i(\epsilon''_d) \geq N_{BWL}\,, \quad (12)$$

where i stands for trues or randoms. Here, $N_{tot}(\epsilon''_d)$ is the total rate presented to the coincidence processor by the buckets and is given by:

$$N_{tot}(\epsilon''_d) = N_t(\epsilon''_d) + 2N_r(\epsilon''_d)\,. \quad (13)$$

This total rate explicitly assumes that randoms are acquired in a prompt and delayed coincidence window. It is also divided by a number, n_{proc}, of coincidence processors that may be running in parallel.

D. Validation of the Model

The realism of this simple model may be evaluated by comparing its predictions to the rates measured with a uniformly active water filled phantom of 20 cm diameter and 20 cm length in the FOV of the ECAT-953B [3] and EXACT HR PLUS [6]. The second and third columns of

Table 1 give the input values adopted to describe these scanners operated in 3-D mode. A one letter tag appears with the parameter symbol in the first column to indicate whether its value is specified (s), calculated (c), or fitted to the data (f). Specified values could be found from details of the 953B or HR PLUS designs available in the literature [3, 4, 5] or directly from the manufacturer [6]. The only fitted parameter is ϵ_{thr}.

Parameter		953B	HR+(BGO)	HR+(LSO)
$\epsilon_d(\%)$	c	94.4	94.4	91.8
R_{ph} (cm)	s	10	10	10
L_{ph} (cm)	s	20	20	20
Z_d (cm)	s	10.7	15.2	15.2
R_d (cm)	s	38	41.3	41.3
P_s^0	c	0.3730	0.3628	0.3397
P_s^1	c	0.0974	0.1166	0.1092
P_t^0	c	0.1021	0.0960	0.0836
P_t^1	c	0.0654	0.0489	0.0432
n_{buck}	s	12	24	24
n_{excl}	s	7	19	19
n_{pair}	s	30	60	60
n_{tripl}	s	200	0	0
τ_{coinc} (ns)	s	12	12	12
$\epsilon_{thr}(\%)$	f	87	89	89
τ_{block} (ns)	s	700	700	80
n_{block}	s	96	288	288
n_{ring}	s	2	1	1
n_{blbk}	s	4	12	12
τ_{buck} (ns)	s	256	256	256
τ_{proc} (ns)	s	256	0	0
n_{proc}	s	4	1	1
$N_{BW\,L}$ (MHz)	s	1.95	2.6	2.6

Table 1: Input parameters to the count rate model along with their specified or estimated values for the ECAT-953B, the EXACT HR PLUS and a hypothetical EXACT HR PLUS made of LSO.

A Monte Carlo simulation [7] was used to evaluate the values of the survival probability factors P_s^0, P_s^1, P_t^0, and P_t^1. These were simply computed by counting the number of single and coincident photons generated in the phantom and reaching the detectors in the presence or absence of Compton scattering in its volume. Photoelectric absorption in the phantom was neglected. The values also account for the energy resolution and a lower discriminator threshold of 380 keV in the 953B [3] and 350 keV in the HR PLUS [6]. In the case of the LSO based EXACT HR PLUS, values of the survival probabilities were computed by replacing BGO with LSO in the simulation.

Figure 1(a) compares, as a function of specific activity, the measured count rate performances of the the ECAT-953B to those predicted by the model. The data are borrowed from Ref. [3]. The only free parameter, ϵ_{thr}, was adjusted to match the measured true count rate at low specific activity. A good agreement was obtained with $\epsilon_{thr} = 87\%$. As the impact of energy thresholding is included in the scattering survival probabilities, this value accounts for the packing fraction of the scanner. Once ϵ_{thr} is fixed, the rates of true, random and multiple events are entirely constrained. The agreement is very good given the simplicity of the model and the availability of only one free parameter.

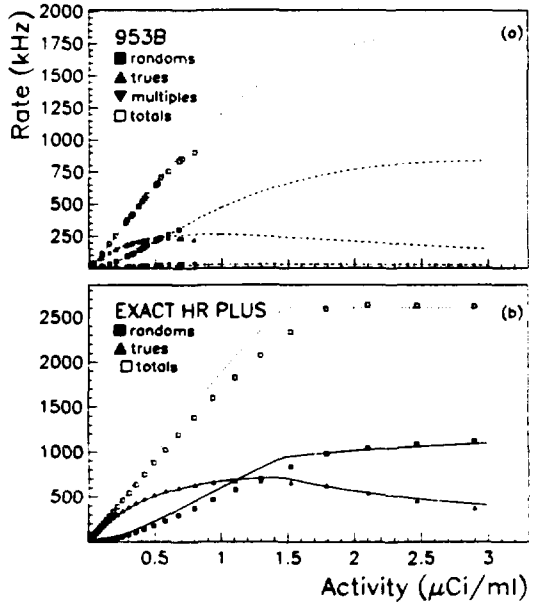

Figure 1: Comparison of measured (symbols) and predicted (lines) count rate performances for the ECAT-953B (a) and the HR PLUS (b).

Figure 1(b) compares the measured rates in the EXACT HR PLUS to those predicted by the model. The data is from Ref. [6]. For the EXACT HR PLUS, the measured true count rate at low activity is best matched with $\epsilon_{thr} = 89\%$. Unlike its account of the 953B, the model is at a loss to fit the measured performances of the EXACT HR PLUS. However, as it overestimates the scanner's random to true ratio, the model's predictions of the peak NEC rate and saturation activity will be pessimistic. In absence of a perfect fit, this bias is taken as acceptable since it only brings conservatism to our conclusions. The uncertainty will also be shown to be small in the next section.

III. Using LSO for the HR PLUS

Figure 2 shows the predicted evolution of the NEC rate from a BGO to LSO made HR PLUS with bucket processing periods of $\tau_{buck} = 256$, 128 and 64 nsec. Input parameters necessary to model the LSO scanner are given in Table 1. For the full lines, the saturation bandwidth N_{BWL} was kept to its specified value of 2.6 MHz. For the dashed lines, N_{BWL} was set to 1 GHz, well above the total count rate at saturation of the NEC when using τ_{buck} of 128 and 64 nsec. Here, the NEC was calculated as:

$$\mathrm{NEC} = \frac{[n'_{unscat}(\epsilon''_d)]^2}{n'_{unscat}(\epsilon''_d) + n'_{scat}(\epsilon''_d) + 2n'_r(\epsilon''_d)}. \qquad (14)$$

The expression applies only to the total rate of true events, and carries an extra factor of 2 for the statistical noise on

the randoms acquired by the delayed coincidence window.

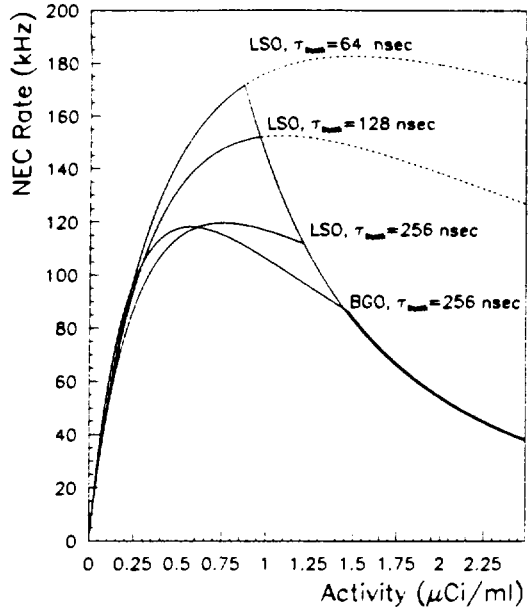

Figure 2: Calculated NEC curves for the BGO and LSO made HR PLUS with bucket processing periods of τ_{buck} = 256, 128 and 64 nsec.

Comparing first the BGO and LSO made HR PLUS operating with the nominal bucket period of 256 nsec indicates a marginal gain on the peak NEC rate from the exchange BGO → LSO. This is not surprizing as using LSO does not improve the scanner's sensitivity and the timing specifications of the buckets and coincidence processor are kept unchanged. The reduction in event losses achieved in using τ_{block} = 80 nsec, to exploit the faster decay time of LSO, only increases the peak NEC value from 118 to 120 kHz, while the corresponding saturation activity raises from 0.57 to 0.76 μCi/ml.

The model's bias in predicting these absolute values was estimated by enforcing a fit between the predicted and measured random rates. An *ad hoc* fit to the random rate was achieved in arbitrarily reducing by 9% the values of P_s^0 and P_s^1 listed in the third column of Table 1. The peak NEC value predicted for the HR PLUS was then found to reach a value of 136 kHz at a saturation activity of 0.65 μCi/ml. Thus, without *ad hoc* correction, the model seems to be pessimistic by 15% in its predictions of the HR PLUS performances and as such is understood to be conservative.

Additional gains to the maximum NEC of an LSO made HR PLUS can be achieved by reducing the event losses at the bucket level. This can be done by either reducing the number of block detectors per bucket, n_{blbk}, or alternatively by reducing the processing clock period, τ_{buck}. Figure 2 shows the resulting gains for bucket clock cycles of 128 and 64 nsec. Comparing the full and dashed lines immediately shows that the NEC does not reach its maximum with faster buckets unless the saturation bandwidth of the data acquisition system, N_{BW_L}, is also increased. The limit is set by the randoms which rapidly overrun the trues to dominate the available bandwidth. For bucket cycles of τ_{buck} = 128 (64) nsec, the NEC will reach a maximum of 152(182) kHz at an activity of 1.09 (1.51) μCi/ml provided the data acquisition bandwidth is higher than N_{BW_L}=3.1 (5.8) MHz.

The suppression of random events through a reduction of the coincidence window also counts among the immediate ways of improving the maximum NEC rate reached in an LSO based tomograph. In Ref. [8], the full-width-at-half-maximum (FWHM) timing resolution achieved with a small LSO crystal coupled to a phototube was measured to be 400 psec using a ^{60}Co source and a 100 keV threshold. From this result, one may expect a lower limit of 900 psec FWHM for the coincidence timing resolution of two LSO block detectors subject to 511 keV photons. In absence of time-of-flight (TOF) information, the coincidence window width, τ_{coinc}, can then be brought down to 5 nsec. This setting will achieve optimal random suppression while not yet cutting the trues in the HR PLUS with a FOV diameter as large as 45 cm. Operating the scanner in head mode only, with a FOV diameter of 25 cm, would allow the use of τ_{coinc}=4 nsec.

Figure 3 presents the calculated maximum NEC rate and saturation activities reached in an LSO based HR PLUS as a function of the coincidence window width, τ_{coinc}, from 4 to 12 nsec. The data points computed with τ_{coinc}=4 nsec are shown with dashed lines as they may only be reached in head mode or if the time resolution of LSO blocks eventually proves to be lower than our estimated 900 psec. The results are also presented for clock periods of τ_{buck}=256, 128 and 64 nsec to see the joint impact of improving the buckets. The results were obtained by assuming a saturation bandwidth, N_{BW_L} of 1 GHz. All other inputs to the model are in accordance to the values in the last column of Table 1.

The results readily indicate the significant increase of the peak NEC achieved by exploiting the superior timing resolution of LSO. Considering buckets operating at τ_{buck} = 128 nsec and a coincidence window width of 5 nsec, one realises an increase of a factor 2.2 of the peak NEC rate in an LSO made HR PLUS over its BGO parent. The saturation activity increases accordingly by a factor 2.7. Operating with these specifications requires the handling of a total rate of 2.9 MHz, only 0.3 MHz more than the saturation bandwidth of the actual HR PLUS scanner. When buckets on a 64 nsec cycle are considered, the NEC rate reaches a maximum of 331 kHz, to be 2.8 times higher than in the BGO scanner. Under these specifications, the NEC saturates at an activity of 2.22 μCi/ml, with a total event rate of 5.38 MHz presented to the front-end data acquisition system.

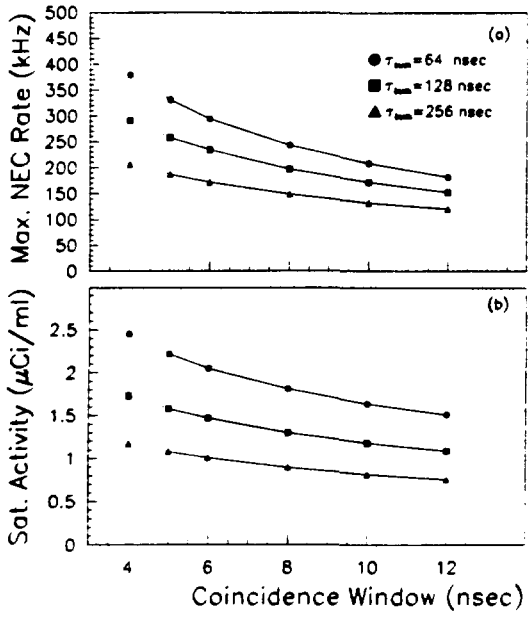

Figure 3: (a) Calculated maximum NEC rate as a function of the coincidence window width and three possible bucket clock periods in an EXACT HR PLUS with LSO. (b) Calculated values of corresponding saturation activities as a function of the coincidence window width.

IV. Discussion and Conclusions

The prime motivation for this work was to conduct a comprehensive and quantitative evaluation of the immediate benefits in implementing LSO made detectors in state-of-the-art PET scanners. Our analysis was based on a simple model which proved to fit well the measured count rate performances of Siemens-CTI's ECAT-953B and to be 15% conservative in predicting the peak NEC rate of the EXACT HR PLUS. Despite its conservatism on the HR PLUS absolute NEC performances, this analysis brings firsthand quantitative answers on the impact of using LSO in modern PET scanners. The results indicate that only replacing BGO by the faster LSO in the HR PLUS design will not lead to any increase of its NEC rate. Significant gains simultaneously call for a reduced coincidence window width, faster bucket processing cycles and a larger bandwidth of the data acquisition system. We found that one can count on an increase of the HR PLUS peak NEC by a factor 2.2 in using a 5 nsec wide coincidence window, buckets on a 128 nsec clock cycle, and a front–end data acquisition that can sustain a total rate of 2.9 MHz.

Hopefully, such specifications are well within technical reach and can be implemented at the cost of a moderate design upgrade. Indeed, reducing the coincidence window width to 5 nsec and increasing the total event rate capacity by 300 extra kHz should be straightforward. Halving the buckets' clock cycle also appears to be a realistic goal. Practically, this just amounts to doubling the number of bucket boards, each handling half the actual number of detectors processed by a bucket in the HR PLUS. This first solution could however bring a real estate problem on the gantry. In that case, one could speed up the buckets by using commercially available analog-to-digital converters that offer a 12-bit resolution at a throughput rate of 10 Mega samples per second.

Doubling the peak NEC only represents an immediate milestone in exploiting the full potentials of LSO for PET. Given the moderate extra relative gain on the NEC, striving for faster buckets and a larger total event bandwidth appears somewhat unappealing. However, a 5 nsec coincidence window does not fully exploit the timing resolution of LSO and forbids additional gains on the NEC through random suppression. Getting the best out of LSO seems to call for the addition of TOF information to the coincidence logic.

V. Acknowledgments

The authors are grateful to M. E. Casey of Siemens-CTI for knowledgeable discussions on the architecture of the ECAT-953B and EXACT HR PLUS scanners as well as for providing count rate performance data for the EXACT HR PLUS. Christian Moisan acknowledges "Les Fonds pour la Formation des Chercheurs et l'Assistance à la Recherche" for their support through a postdoctoral fellowship.

VI. References

[1] E. Tanaka *et al.*, "Analytical Study of the Performance of a Multilayer Positron Computed Tomography Scanner", J. Comput. Assit. Tomogr., **6(2)** 350, (1982).

[2] L. Eriksson, *et al.* "A Simple Data Loss Model for Positron Camera Systems", IEEE Trans. Nucl. Sci., **NS-41** 1566 (1994).

[3] T.J. Spink *et al.*, "Physical performance of a positron tomograph for brain imaging with retractable septa", Phys. Med. Biol., **37**, No. 8, 1637 (1992).

[4] M. E. Casey, "An Analysis of Counting Losses in Positron Emission Tomography", Ph.D. thesis dissertation, University of Tennessee, Knoxville, December 1992.

[5] J. W. Young *et al.*, "Optimum Bandwidth Usage in Digital Coincidence Detection for PET", In the conference record of the 1993 IEEE Nuclear Science Symposium and Medical Imaging Conference of San Francisco, California, 1205-1208 (1993).

[6] M. E. Casey, Siemens-CTI, private communication.

[7] C. Moisan *et al.*, "A Monte Carlo Study of the Acceptance to Scattered Events in a Depth Encoding PET Camera", IEEE Trans. Nucl. Sci., **NS-43**, 1974 (1996)

[8] T. Ludziejewski *et al.*, "Advantages and Limitations of LSO Scintillator in Nuclear Physics Experiments", IEEE Trans. Nucl. Sci., **NS-42** 328 (1995).